Theor Chem Acc (2006) 116: 614–620
DOI 10.1007/s00214-006-0107-3

REGULAR ARTICLE

I. Martín · E. Mayor · A. M. Velasco

Similarities in the intensities of analogous Rydberg–Rydberg transitions in the molecular series CF_xCl_y ($x = 3, 2, 1; y = 1, 2, 3$)

Received: 03 November 2004 / Accepted: 21 February 2005 / Published online: 22 February 2006

Abstract In this work, the photoabsorption behaviour of the molecular series CF_3Cl, CF_2Cl_2 and $CFCl_3$, involving their ground state and two different Rydberg series, has been studied. The discrepancies or similarities in the intensities of homologous transitions in the three CF_xCl_y molecules have been analysed on account of their electronic structure. Absorption oscillator strengths have been calculated with the Molecular quantum defect orbital (MQDO) approach. Electronic transitions between states belonging to two different unperturbed Rydberg series of the same molecule have been calculated by us for the first time. The quality of the achieved oscillator strengths has been assessed by comparison with, to our knowledge, scarce experimental data available in the literature, through analysis of the discrepancies or similarities in the intensities of homologous transitions in the molecular series CF_xCl_y when states of different type are involved, and by testing the compliance of regularities by the Rydberg series object of our study.

Keywords Molecular series CF_3Cl · CF_2Cl_2 · $CFCl_3$ · Homologous Rydberg–Rydberg transitions · Oscillator strengths · MQDO approach

1 Introduction

Chlorofluoromethanes, such as CCl_3F, CF_2Cl_2, CF_3Cl, which are typical aerosol propellants and refrigerants, have attracted great attention in the field of atmospheric chemistry. They are responsible for the destruction of stratospheric ozone by the Cl radicals released from the photolysis of halogenated methanes, like the above by sunlight [1]. These compounds have also proved to be useful in semiconductor industry, where they play a relevant role in dry and plasma etching.

The absorption spectra of CCl_3F, CF_2Cl_2 and CF_3Cl, also known as CFC-11, CFC-12 and CFC-13, respectively, have been the object of some experimental measurements, particularly in the context of atmospheric photochemistry. We find it important to understand in some detail the photoabsorption and photolysis these compounds undergo in the atmosphere, so that their overall dynamics may be understood better. The key role molecular states of Rydberg type play in UV photochemistry is a well-known [2].

Rydberg states are highly excited electronic states (large n values) that follow very closely the Rydberg progression of energies. Most properties of Rydberg states, in atoms and molecules, vary very rapidly with the principal quantum number, n, typically as an integer power of n [3,4]. For example, the classical radius of the electron orbit, the binding energy and the energy spacing between adjacent Rydberg states scale as n^2, n^{-2}, n^{-3}, respectively, to mention a few relevant features [3].

A comparison between the intensities of homologous electronic transitions along the molecular series CF_xCl_y ($x =$ 1–3; $y =$ 3–1) offers, in our view, physical interest, as it may enable one to follow the changes in the electronic structure and characteristics of the excited states of the molecular series as chlorine atoms are replaced by fluorine atoms. ESCA measurements [5] indicate that when a strongly electronegative atom is present in a molecule, the electron cloud is shifted in such a way that a more positive environment is created around the other atoms. As a consequence, the electrons on these atoms become more closely bound to the molecular core, and their ionisation energies (IPs) increase. Malrieu [2] also remarks that, for a lone-pair-containing polyatomic molecule (involving "heavy" atoms, such as chlorine), the lowest Rydberg states are generated from the pure p lone pairs located on chlorine. This may give rise to similarities in the intensities of transitions that can be correlated in the isolated Cl atom and in the CF_xCl_y molecules.

In the molecules of the present study, this means that the gradual replacement of chlorine with the more electronegative

---

Article for the special issue dedicated to J.-P. Malrieu

I. Martín(✉)· E. Mayor · A. M. Velasco
Departamento de Química Física y Química Inorgánica, Facultad de Ciencias, Universidad de Valladolid,47005 Valladolid, Spain
Tel.:+34-983423272
Fax:+34-983423013
E-mail: imartin@qf.uva.es

Table 1 Values of non-zero angular factors $Q\{a \rightarrow b\}$

C_{3v} symmetry group
$Q\{np\mathrm{e}(\bar{\chi}) \rightarrow ns\mathrm{a}_1(^1\mathrm{E})\} = Q\{np(\mathrm{a}_1, \mathrm{e})(^1\mathrm{A}_1, {}^1\mathrm{A}_2, {}^1\mathrm{E}) \rightarrow ns\mathrm{a}_1(^1\mathrm{E})\} = 1/3$
$Q\{ns\mathrm{a}_1(^1\mathrm{E}) \rightarrow np\mathrm{a}_1(^1\mathrm{E})\} = 1/3$
$Q\{ns\mathrm{a}_1(^1\mathrm{E}) \rightarrow np\mathrm{e}(^1\mathrm{A}_1, {}^1\mathrm{A}_2, {}^1\mathrm{E})\} = 2/3$
C_{2v} symmetry group
$Q\{np\mathrm{b}_2(\bar{\chi}) \rightarrow ns\mathrm{a}_1(^1\mathrm{B}_2)\} = Q\{np(\mathrm{a}_1, \mathrm{b}_1 \text{ or } \mathrm{b}_2)(^1\mathrm{A}_2, {}^1\mathrm{B}_1, {}^1\mathrm{B}_2) \rightarrow ns\mathrm{a}_1(^1\mathrm{B}_2)\} = 1/3$
$Q\{ns\mathrm{a}_1(^1\mathrm{B}_2) \rightarrow np(\mathrm{a}_1, \mathrm{b}_1 \text{ or } \mathrm{b}_2)(^1\mathrm{A}_2, {}^1\mathrm{B}_1, {}^1\mathrm{B}_2)\} = 1/3$

fluorine may cause significant rearrangements in their electron clouds. If so, the excitation energies from the ground configuration to the molecular Rydberg states could become gradually higher and consequently the corresponding electronic transitions would gradually become weaker from CCl_3F to CF_3Cl. On the other hand, the intensity of transitions between two different Rydberg states would be practically unaffected. This is because of the long mean distance of a Rydberg electron from the molecular core. In fact, one of the goals of the present work is to analyze the extent to which the intensities of analogous transitions originating in the molecular ground state or in a given Rydberg state and ending in a Rydberg state (obviously, different from the initial state) exhibit a variation as the chlorine content diminishes along the molecular series CF_xCl_y. Henceforth, we have undertaken the study of the two aforementioned kinds of transitions. The molecular quantum defect orbital (MQDO), that has proven to yield correct intensities for ground–Rydberg transitions [6–13] in a variety of molecular species, has been adopted for the present calculations of absorption oscillator strengths, which are a form of representing the intensities of transitions. The few experimental data on intensities found in the literature are given as *f*-values. The quality of our results will be assessed through several indicators. The ground - Rydberg transition intensities are expected to change noticeably from one molecule to the next, because the ground state molecular orbitals (MO's) will be most affected by the variations in the charge distribution as chlorine atoms are gradually replaced by fluorine atoms along the molecular series CF_xCl_y. Unlike this behaviour, the transitions involving analogous Rydberg states should not be expected to exhibit substantial differences, for the above mentioned reasons. As a third indicator we have chosen to perform an analysis of the regularities that the individual Rydberg series display as the excitation energy increases, given that none of those involved in the present calculations is subject to valence, Rydberg mixing, or any other perturbation. Finally, a comparison, has been made with the intensities calculated for the isolated chlorine atom in transitions that may be correlated to those in the molecules.

2 Computational procedure

The MQDO approach, formulated to deal with molecular Rydberg transitions has been described in detail elsewhere [8]. Thus, only a brief summary of the method will follow. The MQDO radial wavefunctions are the analytical solutions of a one-electron Schrödinger equation that contains a model potential of the form

$$V(r)_a = \frac{(c - \delta_a)(2l + c - \delta_a + 1)}{2r^2} - \frac{1}{r}, \qquad (1)$$

where a represents the set of quantum numbers and symmetry symbols that define a given molecular orbital (MO). The analytical solutions of this equation are related to Kummer functions. In Eq. (1), c is an integer chosen, within a small range of allowed values, to ensure the normalisation of the orbitals and their correct nodal pattern. The quantum defect, δ_a, gives an account of the interaction of the valence and excited MOs with the molecular core. It is related to the energy eigenvalue of the corresponding state through the well-known expression,

$$E_a = T - \frac{1}{2(n_a - \delta_a)^2}, \qquad (2)$$

where T is the ionization energy. Both T and E_a are expressed here in Hartrees. The angular parts of the MQDOs are symmetry-adapted linear combinations of spherical harmonics, in a way such that the complete MOs form bases for the different irreducible representations of the molecular symmetry group.

The absorption oscillator strength for a transition between two bound states a and b may be expressed as,

$$f(a \rightarrow b) = N2/3(E_b - E_a)Q\{a \rightarrow b\}|Rab|^2. \qquad (3)$$

In Eq. (3), N is the number of equivalent electrons in the MO where the transition originates, and $Q\{a \rightarrow b\}$, referred to as the angular factors, result from the integration of the angular part of the transition integral through the usual Racah algebra. The radial transition moment adopts the standard form for electric dipole-allowed transitions,

$$R_{ab} = \langle R_a(r)|r|R_b(r)\rangle. \qquad (4)$$

All the transitions under study have been considered to take place through the electric dipole (E1) mechanism. The radial transition moments (4), within the MQDO model, result in closed-form analytical expressions, which offer, in our view, an important computational advantage. The detailed algebraic expressions are given in in Ref.9 as generalised for bound-bound transitions in molecules.

The values of $Q\{a \rightarrow b\}$ for the symmetry group C_{3v}, to which the Rydberg states of CF_3Cl and $CFCl_3$ belong, together with those for the C_{2v} group, because the Rydberg states of CF_2Cl_2 exhibit this symmetry, are collected in Table 1. In this and in the remaining tables we employ a notation for the molecular Rydberg states that is commonly found in the literature. The *nl* symbol of the atomic orbital to which the Rydberg MO can be correlated is followed by the symbol of the irreducible representation to which the Rydberg orbital belongs within the molecular symmetry group and, in parentheses, by the corresponding molecular term symbol and spin multiplicity.

3 Results and analysis

The ground state electronic configurations, in the independent particle model, of the molecular series Rydberg electron to the molecular core ($x = 3$–1, $y = 1$–3) may be written as [14,15]:
CF_3Cl:
Inner shells: $(\mathrm{Cl}\ 1s)^2(\mathrm{F}\ 1s)^2\ (\mathrm{C}\ 1s)^2(\mathrm{Cl}\ 2s)^2\ (\mathrm{Cl}\ 2p)^6$
Valence shells: $(1a_1)^2(1e)^4\ (2a_1)^2\ (3a_1)^2\ (2e)^4\ (4a_1)^2\ (3e)^4\ (4e)^4\ (1a_2)^2\ (5a_1)^2\ (5e)^4 : X^1\ A_1$
CF_2Cl_2:
Inner shells: $(\mathrm{Cl}\ 1s)^4\ (\mathrm{F}\ 1s)^4\ (\mathrm{C}\ 1s)^2\ (\mathrm{Cl}\ 2s)^4\ (\mathrm{Cl}\ 2p)^{12}$
Valence shells: $(1a_1)^2\ (1b_1)^2\ (2a_1)^2\ (1b_2)^2\ (3a_1)^2\ (2b_2)^2\ (4a_1)^2\ (2b_1)^2\ (5a_1)^2\ (1a_2)^2\ (3b_1)^2\ (3b_2)^2\ (6a_1)^2\ (2a_2)^2\ (4b_1)^2\ (4b_2)^2 : X^1A_1$
$CFCl_3$:
Inner shells: $(\mathrm{Cl}\ 1s)^6\ (\mathrm{F}\ 1s)^2\ (\mathrm{C}\ 1s)^2\ (\mathrm{Cl}\ 2s)^6\ (Cl\ 2p)^{18}$
Valence shells: $(1a_1)^2\ (2a_1)^2\ (1e)^4\ (3a_1)^2\ (4a_1)^2\ (2e)^4\ (3e)^4\ (5a_1)^2\ (4e)^4\ (5e)^4\ (1a_2)^2 : X^1\ A_1$

The HOMO, in the three studied clorofluoromethanes, is essentially a $3p$ lone pair centered on the chlorine atom [14, 15]. The ionization energies (IP's) of the outermost valence electrons adopted in the present calculations have been determined by high resolution HeI and HeII photoelectron spectroscopy (PES) by Cvitas et al. [14]. The energy data chosen for the Rydberg states are the experimental values measured by Au et al. [16] for CF_3Cl. In the case of CF_2Cl_2, experimental values reported by Ibuki et al. [17] from a highly resolved photoabsorption spectrum, have been employed; and for $CFCl_3$, use has been made of the experimental values determined by King and McConkey [18]. Table 2 displays the quantum defects and IPs, for the different Rydberg states of the three studied species, together with those for the isolated Cl atom [19]. Inspection of Table 2 reveals substantial similarities in the magnitude of the quantum defects of the four species, as could be expected, because the Rydberg orbitals of the three molecular species are essentially lone-pair atomic orbitals centered on Cl in its ground state [2,20]. For higher Rydberg states, the energy has been extrapolated through the quantum defect formula given in Eq. (2), as the quantum defects along an unperturbed Rydberg series, characterised by a given angular momentum, and belonging to a particular irreducible representation, exhibit a very nearly constant value. In this form, we have been able to predict intensities for transitions that have not been observed experimentally.

Table 2 Quantum defects corresponding to the different Rydberg states studied in the present work; I.P for the molecular series CF_xCl_y ($x =$ 3–1, $y =$ 1–3) and for the Cl atom

Rydberg state	CF_3Cl^a	$CF_2Cl_2^b$	$CFCl_3^c$	Cl^d
4s	1.99	1.97	1.89	2.09
5s	1.96	1.97	1.89	2.08
4p	1.63	1.65	1.63	1.68
5p	1.63	1.65	1.63	1.68
I.P(eV) [e]	13.08	12.26	11.73	12.96

[a] Au et al. [16]
[b] Ibuki et al. [17]
[c] King et al. [18]
[d] Bashkin et al. [19]
[e] Cvitas et al. [14]

In Table 3, the MQDO calculated absorption oscillator strengths for the ground state-Rydberg state homologous electronic transitions in CF_3Cl, CF_2Cl_2 and $CFCl_3$, that is, $5e\ (X^1A_1) \rightarrow nsa_1(^1E)$, $4b_2(X^1A_1) \rightarrow nsa_1(^1B_2)$, $1a_2\ (X^1A_1) \rightarrow nsa_1(^1A_2)$ ($n = 4$–10), respectively, are collected. As expected, the changes in the molecular core electron density induced by the gradual increase in chlorine content from CF_3Cl to $CFCl_3$, are reflected in the decreasing intensities achieved for analogous transitions.

In the groups of transitions collected in Table 3, all of the type $3p\Gamma(X^1A_1) - nsa_1(^1E)$; $-nsa_1(^1B_2)$; and $-nsa_1(^1A_2)$ ($n = 4$–10), respectively, a gradual decrease in the oscillator strengths along the molecular series CF_xCl_y ($x = 3$–1, $y = 1$–3), for a given value of " n", that is for homologous transitions, is apparent. This decrease is more noticeable in the strongest transitions, which almost concentrate all the intensity of the spectral series. For the weak transitions observed at large values of " n", that is, at rather higher transition energies, the above effect becomes negligible. This feature, particularly in regard to the stronger transitions in a Rydberg series, confirms what could be predicted on the basis of the distribution of charge variations in the molecular ground state as the chlorine content augments. That is, the valence orbitals become more diffuse with increasing chlorination. Moreover, the larger size of the valence shell (as a result of the larger chlorine content) also gives rise to a lower average charge density [26]. This decrease in charge density is reflected in a decrease of the oscillator strengths in the corresponding transitions.

The experimental oscillator strengths reported in the literature, all of them referring to transitions that originate in the molecular ground state, are collected in Table 4. No data obtained through theoretical calculations seem to be available. The technical difficulties involved in the calculation of electronic transitions to molecular Rydberg states is broadly recognised for several ab initio procedures. A few comments regarding a comparison between the presently calculated and the experimental oscillator strengths, displayed in Table 4, will follow.

The presently calculated *f*-value for the $3pe(X^1A_1) \rightarrow 4sa_1(^1E)$ transition of CF_3Cl conforms fairly well with the most recent result reported for this molecule (0.1625 ± 0.032), measured by Au et al. [16] with a high-resolution dipole (e,e) technique, as well as with the *f*-value reported by Suto and Lee [21] (0.1516 ± 0.015). King and McConkey [18] obtained

Table 3 Molecular quantum defect orbital (MQDO) absorption oscillator strengths for analogous ground–Rydberg state transitions in the molecular series CF_xCl_y ($x = 3$–1, $y = 1$–3)

Transition	CF_3Cl	Transition	CF_2Cl_2	Transition	$CFCl_3$
$3pe(X^1A_1)$–$4sa_1(^1E)$	0.1191	$3pb_2(X^1A_1)$–$4sa_1(^1B_2)$	0.0673	$3pa_2(X^1A_1)$–$4sa_1(^1A_2)$	0.0459
$3pe(X^1A_1)$–$5sa_1(^1E)$	0.0224	$3pb_2(X^1A_1)$–$5sa_1(^1B_2)$	0.0145	$3pa_2(X^1A_1)$–$5sa_1(^1A_2)$	0.0110
$3pe(X^1A_1)$–$6sa_1(^1E)$	0.0087	$3pb_2(X^1A_1)$–$6sa_1(^1B_2)$	0.0056	$3pa_2(X^1A_1)$–$6sa_1(^1A_2)$	0.0043
$3pe(X^1A_1)$–$7sa_1(^1E)$	0.0043	$3pb_2(X^1A_1)$–$7sa_1(^1B_2)$	0.0027	$3pa_2(X^1A_1)$–$7sa_1(^1A_2)$	0.0022
$3pe(X^1A_1)$–$8sa_1(^1E)$	0.0024	$3pb_2(X^1A_1)$–$8sa_1(^1B_2)$	0.0015	$3pa_2(X^1A_1)$–$8sa_1(^1A_2)$	0.0012
$3pe(X^1A_1)$–$9sa_1(^1E)$	0.0015	$3pb_2(X^1A_1)$–$9sa_1(^1B_2)$	0.0010	$3pa_2(X^1A_1)$–$9sa_1(^1A_2)$	0.0008
$3pe(X^1A_1)$–$10sa_1(^1E)$	0.0010	$3pb_2(X^1A_1)$–$10sa_1(^1B_2)$	0.0006	$3pa_2(X^1A_1)$–$10sa_1(^1A_2)$	0.0005

Table 4 Experimental absorption oscillator strengths for analogous ground–Rydberg state transitions in the molecular series CF_xCl_y ($x = 3$–1, $y = 1$–3)

Molecule	Transition	MQDO	Expt.	Expt.	Expt.	Expt.
CF_3Cl	$3pe(X^1A_1)$–$4sa_1(^1E)$	0.1191	0.1625 ± 0.032^a	0.1516 ± 0.015^b	0.220 ± 0.088^c	0.1503^d
CF_2Cl_2	$3pb_2(X^1A_1)$–$4sa_1(^1B_2)$	0.0673	0.054 ± 0.0081^e	0.044 ± 0.0044^f	0.0360 ± 0.0064^c	0.0296 ± 0.00148^a
$CFCl_3$	$3pa_2(X^1A_1)$–$4sa_1(^1A_2)$	0.0459	0.046 ± 0.0023^a	0.052 ± 0.0104^c	0.0683 ± 0.0102^e	0.131^d

[a] Au et al. [16]
[b] Suto and Lee [21]
[c] King and McConkey [18]
[d] Doucet et al. [23]
[e] Ibuki et al. [17]
[f] Bastien et al. [24]

an oscillator strength (equal to 0.220 ± 0.088), with a zero angle electron energy-loss technique that is about twice as large the one calculated in this work. It should be noted that the large magnitude of this oscillator strength, may, in part be attributed to the normalization performed by King and McConkey [18] to the measurements by Gilbert et al. [20] and to those by Jochims et al. [22]. The latter [22] appear to be systematically higher in magnitude than all the other values found up to date. Finally, the earliest reported *f*-value (of 0.1503) by Doucet et al. [23], does not substantially disagree with our MQDO oscillator strength. The accuracy of the former [23] is difficult to establish because Doucet et al. [23] determined both the extinction coefficient and the bandwidth from a graph.

Important discrepancies among the available experimental data, are observed as far as the $3pb_2(X^1A_1) \rightarrow 4sa_1(^1B_2)$ transition in CF_2Cl_2 is concerned. Our *f*-value appears to conform fairly well with the value (of 0.054 ± 0.0081) determined by Ibuki et al. [17] with synchrotron radiation, and also with the one measured by Bastien et al. [24] (0.044 ± 0.0044), with an electron storage ring and a low-resolution monochromator. It may be pointed out that none of these experimental values have required normalisation through data from other sources. Some other experimental data are those reported by King et al. [18] and Au et al. [16]. King et al. [18], with a zero-angle electron energy loss spectra technique, obtained an *f*-value (of 0.360 ± 0.0064) that is rather higher in magnitude than the present one. The accuracy of this value [18] is linked to the accuracy of the data chosen for normalisation, ±3% [25]. Au et al. [16], made their measurements with high-resolution dipole (e,e) spectroscopy, obtaining in this case an oscillator strength (of 0.0296 ± 0.00148) that is smaller than ours. The absolute oscillator strength scales were determined by normalisation of their relative spectra [17] to the low-resolution absolute data in the smooth continuous region.

For the $3pa_2(X^1A_1) \rightarrow 4sa_1(^1A_2)$ transition of $CFCl_3$, a general good agreement is found between our MQDO result and the experimental ones found in the literature [16–18], and more so if we take into account their estimated uncertainties. Our MQDO result conforms very well with the most recent measurement performed with a high-resolution dipole (e,e) technique by Au et al. [16], (0.046 ± 0.0023). In addition, a good agreement is found with the value (of 0.052 ± 0.0104) obtained by King et al. [18] with a zero-angle electron energy loss spectra technique, and with that measured by Ibuki et al. [17] (0.0683 ± 0.0102) with synchrotron radiation. However, the oscillator strength reported by Doucet et al. [23], (0.131) is higher than the presently calculated value and the other experimental data. This difference possibly arises from target density errors and/or line saturation effects (i.e., bandwidth/linewidth interactions) occurring in the optical measurement [23]. The accuracy of this value is again difficult to establish as both the extinction coefficient and the bandwidth were graphically determined.

In the remaining tables, the presently calculated oscillator strengths for a number of Rydberg–Rydberg transitions, all originating in the same excited MO, in the molecular series CF_xCl_y, are collected. In Tables 5 and 6, oscillator strengths for homologous electronic transitions of the type, $n'p^* \rightarrow nsa_1(^1E)$, $n'p^+ \rightarrow nsa_1(^1B_2)$, and $n'p^* \rightarrow nsa_1(^1A_2)$ ($n' = 4$–5; $n = 4$–11 (Table 5) and 4–12 (Table 6), respectively, occurring in CF_3Cl, CF_2Cl_2 and $CFCl_3$, are collected. The symbols $n'p^*$ and $n'p^+$, explained at the bottom of the tables, refer to molecular Rydberg orbitals with the same excitation energy, but, in some cases, different symmetry. The excited

Table 5 Molecular quantum defect orbital absorption oscillator strengths for analogous Rydberg–Rydberg transitions in the molecular series CF_xCl_y ($x = 3$–1, $y = 1$–3)

Transition	CF_3Cl	Transition	CF_2Cl_2	Transition	$CFCl_3$
$4p^{\mathrm{a}}$–$5sa_1(^1\mathrm{E})$	0.2415	$4p^{\mathrm{b}}$–$5sa_1(^1\mathrm{B}_2)$	0.2396	$4p^{\mathrm{a}}$–$5sa_1(^1\mathrm{A}_2)$	0.2036
$4p^{\mathrm{a}}$–$6sa_1(^1\mathrm{E})$	0.0293	$4p^{\mathrm{b}}$–$6sa_1(^1\mathrm{B}_2)$	0.0293	$4p^{\mathrm{a}}$–$6sa_1(^1\mathrm{A}_2)$	0.0296
$4p^{\mathrm{a}}$–$7sa_1(^1\mathrm{E})$	0.0100	$4p^{\mathrm{b}}$–$7sa_1(^1\mathrm{B}_2)$	0.0100	$4p^{\mathrm{a}}$–$7sa_1(^1\mathrm{A}_2)$	0.0106
$4p^{\mathrm{a}}$–$8sa_1(^1\mathrm{E})$	0.0048	$4p^{\mathrm{b}}$–$8sa_1(^1\mathrm{B}_2)$	0.0048	$4p^{\mathrm{a}}$–$8sa_1(^1\mathrm{A}_2)$	0.0052
$4p^{\mathrm{a}}$–$9sa_1(^1\mathrm{E})$	0.0027	$4p^{\mathrm{b}}$–$9sa_1(^1\mathrm{B}_2)$	0.0027	$4p^{\mathrm{a}}$–$9sa_1(^1\mathrm{A}_2)$	0.0029
$4p^{\mathrm{a}}$–$10sa_1(^1\mathrm{E})$	0.0017	$4p^{\mathrm{b}}$–$10sa_1(^1\mathrm{B}_2)$	0.0017	$4p^{\mathrm{a}}$–$10sa_1(^1\mathrm{A}_2)$	0.0018
$4p^{\mathrm{a}}$–$11sa_1(^1\mathrm{E})$	0.0011	$4p^{\mathrm{b}}$–$11sa_1(^1\mathrm{B}_2)$	0.0011	$4p^{\mathrm{a}}$–$11sa_1(^1\mathrm{A}_2)$	0.0012

[a] $(a_1, e)(^1A_1, ^1A_2, ^1E)$
[b] $(a_1, b_1, b_2^1)(A_2, ^1B_1, ^1B_2)$

Table 6 Molecular quantum defect orbital absorption oscillator strengths for analogous Rydberg- Rydberg transitions in the molecular series CF_xCl_y ($x = 3$–1, $y = 1$–3)

Transition	CF_3Cl	Transition	CF_2Cl_2	Transition	$CFCl_3$
$5p^{\mathrm{a}}$–$6sa_1(^1\mathrm{E})$	0.3449	$5p^{\mathrm{b}}$–$6sa_1(^1\mathrm{B}_2)$	0.3483	$5p^{\mathrm{a}}$–$6sa_1(^1\mathrm{A}_2)$	0.2953
$5p^{\mathrm{a}}$–$7sa_1(^1\mathrm{E})$	0.0426	$5p^{\mathrm{b}}$–$7sa_1(^1\mathrm{B}_2)$	0.0424	$5p^{\mathrm{a}}$–$7sa_1(^1\mathrm{A}_2)$	0.0429
$5p^{\mathrm{a}}$–$8sa_1(^1\mathrm{E})$	0.0147	$5p^{\mathrm{b}}$–$8sa_1(^1\mathrm{B}_2)$	0.0147	$5p^{\mathrm{a}}$–$8sa_1(^1\mathrm{A}_2)$	0.0155
$5p^{\mathrm{a}}$–$9sa_1(^1\mathrm{E})$	0.0072	$5p^{\mathrm{b}}$–$9sa_1(^1\mathrm{B}_2)$	0.0071	$5p^{\mathrm{a}}$–$9sa_1(^1\mathrm{A}_2)$	0.0077
$5p^{\mathrm{a}}$–$10sa_1(^1\mathrm{E})$	0.0041	$5p^{\mathrm{b}}$–$10sa_1(^1\mathrm{B}_2)$	0.0041	$5p^{\mathrm{a}}$–$10sa_1(^1\mathrm{A}_2)$	0.0045
$5p^{\mathrm{a}}$–$11sa_1(^1\mathrm{E})$	0.0026	$5p^{\mathrm{b}}$–$11sa_1(^1\mathrm{B}_2)$	0.0026	$5p^{\mathrm{a}}$–$11sa_1(^1\mathrm{A}_2)$	0.0028
$5p^{\mathrm{a}}$–$12sa_1(^1\mathrm{E})$	0.0018	$5p^{\mathrm{b}}$–$12sa_1(^1\mathrm{B}_2)$	0.0017	$5p^{\mathrm{a}}$–$12sa_1(^1\mathrm{A}_2)$	0.0019

[a] $(a_1, e)(^1A_1, ^1A_2, ^1E)$
[b] $(a_1, b_1, b_2^1)(A_2, ^1B_1, ^1B_2)$

Table 7 Molecular quantum defect orbital absorption oscillator strengths for analogous transitions in the molecular series CF_xCl_y ($x = 3$–1, $y = 1$–3)

Transition	CF_3Cl	Transition	CF_2Cl_2	Transition	$CFCl_3$
$4sa_1(^1\mathrm{E})$–$4p^{\mathrm{a}}$	0.8825	$4sa_1(^1\mathrm{B}_2)$–$4p^{\mathrm{b}}$	0.8422	$4sa_1(^1\mathrm{A}_2)$–$4p^{\mathrm{a}}$	0.7386
$5sa_1(^1\mathrm{E})$–$5p^{\mathrm{a}}$	1.2455	$5sa_1(^1\mathrm{B}_2)$–$5p^{\mathrm{b}}$	1.2353	$5sa_1(^1\mathrm{A}_2)$–$5p^{\mathrm{a}}$	1.0859

[a] $(a_1, e)(^1A_1, ^1A_2, ^1E)$
[b] $(a_1, b_1, b_2^1)(A_2, ^1B_1, ^1B_2)$

states they define may be described by different term values. Likewise, in Table 7, the oscillator strengths for the homologous Rydberg–Rydberg transitions $nsa_1(^1E) \rightarrow n'p^*$, nsa_1 $(^1B_2) \rightarrow n'p^+$, and $nsa_1(^1A_2) \rightarrow n'p^*$ ($n' = 4$–5; $n =$ 4–5), respectively, are displayed. Transitions to higher upper states are not included in Table 7 because the corresponding *f*-values were either negligible or equal to 0. The trend in oscillator strengths for homologous transitions contradicts that in Table 3, but this effect is only important in the stronger transitions of a given spectral series. Already in the second transition ($n = 6$ in Table 5 and $n = 7$ in Table 6), and more so as n becomes greater, the intensities of homologous transitions in the three studied molecules conform generally rather well with each other. According to Gilbert et al. [20], in these molecular series, the Rydberg states belonging to most of the existing Rydberg series in a molecule, are essentially centred around a chlorine atom. This is in accord with the remarks by Malrieu [2] regarding the role played by the chlorine p lone pairs in the generation of the different Rydberg series. Nonetheless, as it happened in the ground- Rydberg transitions of the molecular series (Table 3), the strongest transitions concentrate a good deal of the total intensity in all given spectral series.

We shall next refer to the oscillator strengths calculated for a number of "multiplet" transitions involving *ns* and *np* (n = 4, 5) atomic orbitals of the isolated chlorine atom. The relativistic formulation of the (atomic) RQDO method [27,28] has been used in these calculations. In Table 8, we have grouped the *f*-values for the Cl atom together with the different sets of homologous transitions in the CF_xCl_y ($x = 3$–1, $y = 1$–3) molecules that can be correlated with the "supermultiplet" transitions in Cl (what is known as "supermultiplet" is the group of multiplets with different L-value but the same spin multiplicity that arise from a given electron configuration in an atom [29]). Before comparing the magnitudes of the oscillator strengths in the isolated atom and in the molecules, a few remarks are in order. Given that an atom possesses an infinite symmetry, the atomic states described by a given *nl* pair of orbital and principal quantum numbers, are symmetry-split in the molecule. The consequences of the difference in the number of homologous states in chlorine and in the studied molecules is that a comparison of transition intensities may only be made between the sum of the individual intensities of an nl–$n'l'$ "supermultiplet" in the atom and the sum of the intensities of all the nl–$n'l'$ transitions comprising all the different irreducible representations involved

Table 8 Molecular quantum defect orbital absorption oscillator strengths for analogous transitions in the molecular series CF_xCl_y ($x = 3$–1, $y = 1$–3) and the isolated halogen atom Cl

Transition	Cl	Transition	CF_3Cl	Transition	CF_2Cl_2	Transition	$CFCl_3$
$4p^4P$–$5s^4P$	0.2486	$4p^a - 5sa_1(^1E)$	0.2415	$4p^b$–$5sa_1(^1B_2)$	0.2396	$4p* - 5sa_1(^1A_2)$	0.2036
$4s^4P$–$4p^4$ (S,P,D)	0.9020	$4sa_1(^1E)$–$4p^a$	0.8825	$4sa_1(^1B_2)$–$4p^+$	0.8421	$4sa_1(^1A_2)$–$4p^a$	0.7386
$5s^2P$–$5p^2$ (S,P,D)	1.2626	$5sa_1(^1E)$–$5p^a$	1.2455	$5sa(^1B_2)_1$–$5p^b$	1.2352	$5sa_1(^1A_2)$–$5p^a$	1.0859

$^a(a_1, e)(^1A_1, ^1A_2, ^1E)$
$^b(a_1, b_1, b_2^1)(A_2, ^1B_1, ^1B_2)$

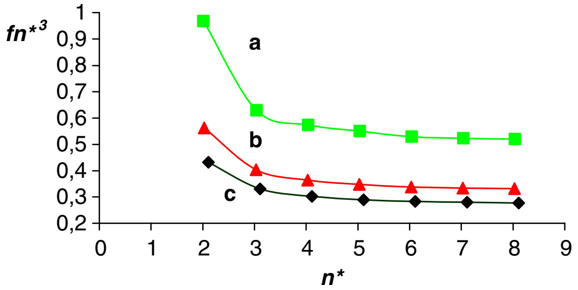

Fig. 1 Systematic trends of the $(X^1A_1) - nsa_1$ ($n = 4 - 10$) transitions along the Rydberg series in CF_xCl_y ($x = 3$–1, $y = 1$–3). **a** CF_3Cl, **b** CF_2Cl_2, **c** $CFCl_3$

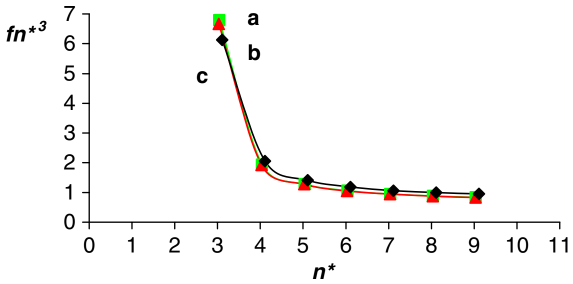

Fig. 2 Systematic trends of the $(4p*, 4p^+) - nsa_1$ ($n = 5$–11), transitions along the Rydberg series in CF_xCl_y ($x = 3$–1, $y = 1$–3). **a** CF_3Cl, **b** CF_2Cl_2, **c** $CFCl_3$

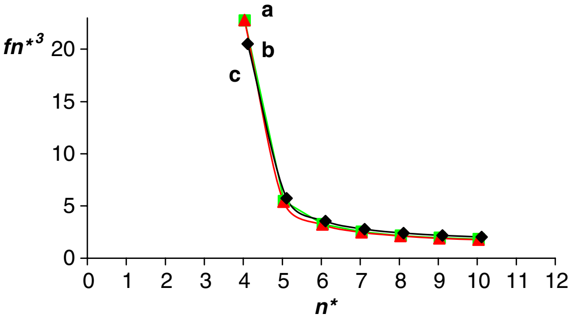

Fig. 3 Systematic trends of the $(4p^*, 4p^+) - nsa_1$ ($n = 6$–12), transitions along the Rydberg series in CF_xCl_y ($x = 3$–1, $y = 1$–3). **a** CF_3Cl, **b** CF_2Cl_2, **c** $CFCl_3$

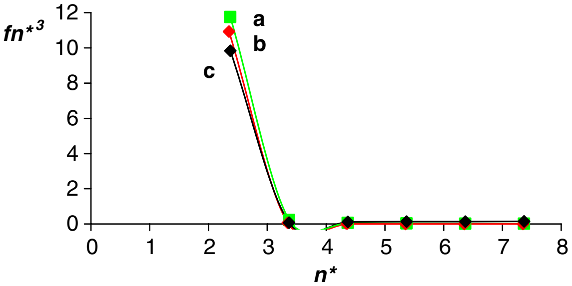

Fig. 4 Systematic trends of the transitions $4sa_1 - (np^*, np^+)$ ($n = 4$–9) along the Rydberg series in CF_xCl_y ($x = 3$–1, $y = 1$–3). **a** CF_3Cl, **b** CF_2Cl_2, **c** $CFCl_3$

(if more than one) in the molecules. The oscillator strengths for these groups of transitions are displayed in Table 8.

An inspection of Table 8 makes apparent a clear similarity among the *f*-values of the three molecular species and that of the chlorine atom, in a given homologous transition. This feature may serve as a further confirmation of the remarks made independently by Malrieu [2] and by Gilbert [20] in the sense that the Rydberg states of the studied molecules mainly arise from the chlorine atoms lone pairs. We interpret the slight but gradual decrease in the magnitude of the oscillator strengths in a given type of transition in going from Cl to $CFCl_3$ in terms of the slight decrease in the quantum defect for the *ns* orbitals in the same direction: $\delta_{ns} = 2.09, 1.99, 1.97 \text{and} 1.89$ for Cl, CF_3Cl, CF_3Cl_2 and $CFCl_3$, respectively. The quantum defect for the *p*-type orbitals, however, exhibits a stable value of about 1.63 in all the above species.

As mentioned in the Introduction, another indicator of the internal consistency and correctness of our results consists of a test on the regularities complied with by the transition intensities along an unerturbed Rydberg series. All the transitions originating in a given state should display a systematic trend along the different Rydberg series formed by the increasingly excited upper states, all, obviously with the same symmetry. It has been long established [29], for all spectral series of the hydrogen atom, as well as for other atoms that presented a “hydrogenic” behaviour, that the square of the radial transition integral (To which the oscillator strength is proportional) displayed the same trend, as *n* increases with excitation along the spectral series as that of the negative third power of the quantum number $(n)^{-3}$ that characterised the upper state, For a non- hydrogenic system (even though the molecular Rydberg orbitals exhibit a near-hydrogenic character, in particular when highly excited), *n* should be replaced by its corresponding “effective quantum number” $n^* = n - \delta$. Compliance with this behaviour at sufficiently high values of n^* is a qualitative proof of the correctness of the oscillator strengths. This is more easily observed if the product $f(n^*)^3$

is plotted aganist n^* along a Rydberg series. A decreasing trend is expected to be found for the first few values of n^*, until the slope becoming practically unchanged as n^*, and, thus, the energy of the upper state, increases [29]. This behaviour is observed in the different Rydberg series presently studied belonging to CF_3Cl, CF_2Cl_2 and $CFCl_3$, as depicted in Figs. 1, 2, 3 and 4. In Fig. 1, which derives from Table 3, the initial state of the transition is the molecular ground state. In the remaining Figs. 2, 3 and 4, the transitions always depart from an excited state. Figures 2 and 3 derive from Tables 5 and 6, respectively. Figure 4 corresponds to spectral series involving Rydberg–Rydberg transitions in the molecular system CF_xCl_y.. These spectral series are also part of the present study although they have not been presented in tables. However, the two corresponding graphs may reinforce through their regularities the internal consistency of the MQDO. approach and, at least the qualitative correctness of the results achieved in the present work.

Acknowledgements The authors wish to express their gratitude to Professor Malrieu for having been a constant source of inspiration and knowledge with his work. The present work has been supported by the D.G.I. of the Spanish Ministry for Science and Technology within Project No. BQU2001-2935-C02, and by European FEDER funds. A. M. V. and E.M. also wish to acknowledge their research agreement and grant from the first institution and from the Spanish Ministry for Education, respectively.

References

1. Molina M-J, Rowland F-S (1975) Rev Geophys Space 13:1
2. Malrieu J-P (1981) Theor Chim Acta 59:251
3. Sttebings R-F, Dunning F-B (1983) Rydberg states of atoms and molecules. Cambridge University Press, Cambridge, p 45
4. Schlag E-W, Levine R-D (1997) Comment At Mol Phys 33:159
5. Siegbahn K, Nordling C, Johansson C, Hedman J, Heden P-F, Hamrin K, Gelius U, Bergmack T, Werme L-O, Manne R, Baer Y (1969) ESCA applied to free molecules. North Holland, Amsterdam, p 104
6. Velasco A-M, Mayor E, Martin I (2003) Chem Phys Lett 377:189
7. Velasco A-M, Mayor E, Martin I (2003) Chem Phys Lett 376:167
8. Martín I, Lavín C, Velasco A-M, Martín M-O, Karwowski J, Diercksen G-H-F (1996) Chem Phys Lett 202:307
9. Martín I, Lavín C, Karwowski J (1996) Chem Phys Lett 255:89
10. Velasco A-M, Martín I, Lavín C (1997) Chem Phys Lett 264:579
11. Mayor E, Velasco A-M, Martín I (2004) J Phys Chem A 108:5699
12. Velasco A-M, Bustos E, Martín I, Lavín C (2002) J Phys Chem A 106:6401
13. Martín I, Mayor E, Velasco A-M (2004) Int J Quant Chem 100:1003
14. Cvitas T, Gusten H, Klasinc L (1977) J Chem Phys 67:2687
15. Potts A-W, Novak I, Quinn F, Marr G-V, Dobson B, Hilier I-H, West J-B (1985) J Phys B: At Mol Phys 18:3177
16. Au J-W, Burton G-R, Brion C-E (1997) Chem Phys 221:151
17. Ibuki T, Hiraya A, Shobatake K (1989) J Chem Phys 90:6290
18. King G-C, McConkey J-W (1978) J Phys B: Atom Molec Phys 11:1861
19. Bashkin S, Stoner J-O (1975)Atomic Energy Levels and Gotrian Diagrams, vols.1, 2. North Holland-American Elsevier, New York (1978)
20. Gilbert R, Sauvageau P, Sandorfy C (1974) J Chem Phys 60:4820
21. Suto M, Lee L-C (1983) J Chem Phys 79:1127
22. Jochims H-W, Lohr W, Baumgärtel H (1976) Ber Bunsenges Phys Chem 80:130
23. Doucet J, Sauvageau P, Sandorfy C (1973) J Chem Phys 58:3708
24. Bastien F, Chatterton P-A, Marode E, Maruzzi J-L (1985) J Phys D:App Phys 18:1327
25. Person J-C, Fawler D-E, Nicole P-P (1975) Argonne National Laboratory report ANL-75–60 Part 1
26. Ying J-F, Leung K-T (1994) J Chem Phys 101:8333
27. Martín I, Karwowski J (1991) J Phys B:Atom Mol Opt Phys 24:1539
28. Karwowski J, Martín I (1991) Phys Rev A 43:4832
29. Martin W-C, Wiese W-L (1996) In: Drake G-W-F (ed) Atomic, molecular, and optical physics handbook. American Institute of Physics, Woodbury